ELSEVIER

PII: S0032-3861(98)00129-3

Polymer Vol. 39 No. 26, pp. 6723–6731, 1998

0032-3861/98/$ - see front matter

The measurement of compositional heterogeneity in a propylene–ethylene block copolymer

Y. Feng and J. N. Hay*
School of Metallurgy and Materials, The University of Birmingham, Edgbaston, Birmingham B15 2TT, UK
(Revised 24 January 1998)

^{13}C nuclear magnetic resonance (n.m.r.) and Fourier transform infra-red (*FT*i.r.) spectroscopies, as well as wide-angle X-ray diffraction (WAXD), differential scanning calorimetry (d.s.c.) and temperature rising elution fractionation (TREF), have been combined to measure the composional heterogeneity of a commercial propylene–ethylene block copolymer. It has been shown that the copolymer contains molecular species with a wide variation in composition, and the copolymer products range from amorphous ethylene–propylene rubbers (EPR) to crystallisable propylene–ethylene statistical copolymers, polyethylene and polypropylene homopolymers as well as blocks of various lengths. The so-called block copolymer was composed of about 15% amorphous EPR, 5% random copolymer, 28% block copolymers with long propylene and long ethylene sequences, and 52% homopolypropylene. The crystallisation and melting behaviour of these fractions have been investigated.

(Keywords: block propylene–ethylene copolymer; compositional heterogeneity; monomer sequence distribution)

INTRODUCTION

Polypropylene, at low temperature, is intrinsically brittle and suffers from embrittlement on ageing close to its glass transition temperature (T_g). Its toughness is improved by blending with a variety of rubbers[1,2], addition of nucleating agent to reduce the average size of the spherulites[3,4] and by copolymerisation with ethylene[5]. There is, however, little published information concerning the compositional variation and molecular structure of commercial propylene–ethylene block copolymers. It is generally considered that the block copolymer is formed in a step polymerisation but, because of transfer reactions, some homopolymer must be present. It is generally accepted that the composition of the block copolymer will be more complicated than that implied by block copolymer[6].

Temperature rising elution fractionation (TREF) has been shown[7] to be a powerful technique for studies of the compositional heterogeneity in polyolefins. The technique relies on the ability of molecules with different composition to crystallise to different extents and at different temperatures. Separation occurs typically by comonomer content, degree of tacticity and number of branch sequence lengths. As prepared by heterogeneous catalysts, most olefins copolymers contain distributions of comonomer units such that different molecular chains possess different proportions of each unit. As a result, chains with fewer non-crystallisable units crystallise at higher temperatures and with a higher degree of crystallinity; consequently they dissolve at higher temperatures than those with more comonomer units. Accordingly, they can be separated by temperature rising elution fractionation[8] under appropriate experimental conditions.

The purpose of this paper is to describe the changes in composition and monomer sequence distribution of a commercial propylene–ethylene block copolymer by using temperature rising elution fractionation (TREF) to separate the copolymer into discrete fractions which can then be characterised individually by ^{13}C nuclear magnetic resonance (n.m.r.) spectroscopy, Fourier transfrom infra-red (*FT*i.r.) spectroscopy, differential scanning calorimetry (d.s.c.) and wide-angle X-ray diffraction (WAXD). This enabled the microstructural variation within each copolymer fraction to be assessed. The crystallisation and melting behaviour of these fractions was also investigated to determine the part played by compositional heterogeneity in the degree of crystallinity and the lowering of the melting point of the copolymers.

EXPERIMENTAL

Temperature rising elution fractionation was carried out on a block PP copolymer sample provided by Solvay. The grade number was RV210 and the ethylene content was about 8%. A preparative TREF system was used, consisting of a jacketed column thermostated to ± 0.1°C by circulating heated oil. The fractionation column, 5 cm in diameter and 1.40 m in length, was made of a large double-walled glass condenser and packed with fine silica sand.

About 3–5 g of polymer was dissolved in 400 cm^3 of xylene at 130°C and stabilised with the antioxidant Santanox R. The solution was eluted through the top third of the TREF column at 130°C, and the column cooled slowly to room temperature over 16 h. This resulted in a gradual deposition of the crystalline copolymer on to the top third of the column packing. The first fractions were eluted at room temperature with xylene and subsequent fractions collected on increasing the temperature stepwise from room temperature to 130°C. The eluted polymer fractions were precipitated into a large excess of methanol at room

* To whom correspondence should be addressed

Table 1 Fractionation of the block copolymer

Fraction no.	Elution temp. (°C)	Weight (± 0.1 mg)	w_i	$C(M_i)$
B1	24	655.5	14.9	7.45
B2	35	90.7	2.1	15.95
B3	52	36.0	0.8	17.40
B4	65	57.9	1.3	18.45
B5	75	26.6	0.7	19.45
B6	85	3.5	0.1	19.85
B7	90	0.0	0.0	19.90
B8	95	1.4	0.0	19.90
B9	100	3.2	0.1	19.95
B10	102	118.6	2.7	21.35
B11	105	779.9	17.8	31.60
B12	107	217.7	5.0	43.00
B13	110	92.7	2.1	46.55
B14	112	300.2	6.8	51.00
B15	115	1405.8	32.0	70.40
B16	117	98.3	2.2	87.50
B17	120	155.7	3.6	90.40
B18	123	345.6	7.9	96.15

Weight of sample used: 5.5 g
Total recovery: 79.8%

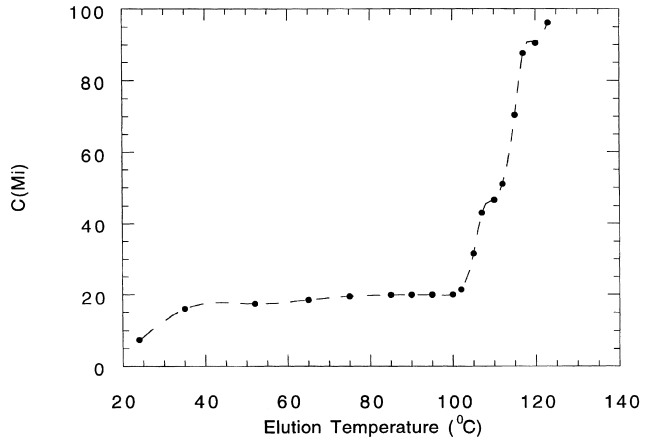

Figure 1 Temperature rising elution fractionation of the block copolymer

temperature, filtered and dried *in vacuo* at 60°C to constant weight.

^{13}C-n.m.r. spectra were measured on a 270 MHz Jeol GX270 FT-NMR Fourier transform ^{13}C-n.m.r. spectrometer. Solutions (10 wt%) were prepared in *o*-dichlorobenzene with 5% deuterated dimethyl sulfoxide as an internal lock. Measurments were made at 130°C. The nomenclature and assignments of the different carbon atoms along the molecular chain adopted for the absorption bands in the n.m.r. spectra were those of Carman and Wilkes[9]. In this, a methylene carbon is identified as *S* with two Greek letters indicating its distance in both directions from the nearest tertiary carbon, e.g. the letter δ indicates a methylene group which is three away from a tertiary carbon. Similarly, a methine carbon is identified as *T* with two Greek letters showing the positions of the nearest tertiary carbons. A methyl carbon is given the letter *P* with two Greek letters that are the same as those for the attached tertiary carbon.

*FT*i.r. spectra were measured with a Mattson Polaris Fourier transform infra-red spectrometer, interfaced to a PCV computer. Compression-moulded films 10–100 mm thick were used in this analysis depending on the absorption band being measured.

Wide-angle X-ray diffraction experiments were carried out on powdered samples at ambient temperature on a Phillips Sie-122 X-ray diffractometer using Ni-filtered Cu K_α radiation, wavelength of 1.54 Å. Typical exposure times were 16 h. Scattered intensities were measured as a function of 2θ values between 5 and 50° at a step size of 0.05°.

D.s.c. experiments were carried out on a Perkin–Elmer model DSC-2 instrument, interfaced to a BBC Master computer via an analogue-to-digital converter. The temperature scale of the calorimeter was calibrated from the melting points of zone-refined stearic acid (m.p. 343.50 K) and highly purified metals such as indium (m.p. 429.78 K), tin (m.p. 505.06 K), lead (m.p. 600.50 K) and zinc (m.p. 692.65 K). The thermal response of the calorimeter was calibrated from the heat of fusion of ultra-pure indium, assuming it to be 28.4 J g^{-1}. Samples were placed in aluminium pans with lids without crimping and an empty aluminium pan and lid used as reference. Corrections were made for the thermal lag in m.p. determinations by extrapolation to zero sample size at constant heating rate, or to zero heating rate at constant sample size. The degree of crystallinity of the polyethylene and polypropylene fractions was determined from the measured heats of fusion determined on the calorimeter, by using appropriate heats of fusion of the 100% crystalline polymers.

RESULTS AND DISCUSSION

Fractionation and characterisation

A block copolymer of propylene–ethylene was fractionated as described above and 18 fractions collected between room temperature and 125°C. The fractionation data are summarised in *Table 1* including the weight fraction, w_i, for the *i*th fraction and the accumulative weight, $C(M_i)$. The accumulative weight–elution temperature distribution, as shown in *Figure 1*, indicates that up to 20% of the copolymer is soluble below 100°C. Except for the fraction obtained at room temperature, most of the fractionation occurred over a narrow temperature region, 100–130°C. The overall distribution curve (*Figure 1*) shows a stepped rather than the more normal s-shaped curves observed previously for linear low-density polyethylenes and polypropylene random copolymers where the fractionation occurred over a wider temperature range.

Table 2 Chemical shifts and intensities for the carbon atoms in propylene–ethylene copolymer in ^{13}C-n.m.r. spectra

Carbon type	Chemical shift (ppm)	Peak intensity (%)				
		B11	B12	B13	B15	B17
$S_{\alpha\alpha}$-CH_2	45.5	20.9	32.2	34.2	24.1	23.3
$S_{\alpha\gamma}$-CH_2	36.8	4.0	0.6	0.7	0.6	0.6
$S_{\alpha\delta}$-CH_2	36.5	2.7	0.6	1.7	0.3	0.4
$S_{\alpha\beta}$-CH_2	—					
$T_{\delta\delta}$-EPE-CH	33.0	1.8	0.3	1.7	0.5	0.7
$T_{\beta\delta}$-EPP-CH	31.5	1.4	0.3	1.0	0.5	1.1
$S_{\gamma\gamma}$-CH_2	31.0	0.0	0.2	0.3	0.0	0.0
$S_{\gamma\delta}$-CH_2	29.5	0.0	0.3	0.3	0.0	0.0
$S_{\delta\delta}$-CH_2	29.0	14.9	7.6	4.3	3.0	0.0
$T_{\beta\beta}$-PPP-CH	28.0	18.7	28.0	29.7	21.0	24.4
$S_{\beta\gamma}$-CH_2	—					
$S_{\beta\delta}$-CH_2	26.5	2.7	0.6	1.7	0.3	0.4
$S_{\beta\beta}$-CH_2	23.5	2.0	0.3	0.3	0.3	0.3
$P_{\beta\beta}$-CH_3-mmPPP	21.0	20.8	26.2	15.7	18.0	16.1
CH_3-mγPPP						
$P_{\beta\delta}$-CH_3-PPE	20.5	2.7	0.6	2.9	2.0	16.5
CH_3-$\gamma\gamma\gamma$PPP						
$P_{\delta\delta}$-CH_3-EPE	19.8	7.4	1.9	5.1	29.3	16.2

Table 2 shows the assignment of the bands, chemical shifts and intensity of each carbon atom in the ^{13}C-n.m.r. spectra of the fractions, from which dyad distributions were determined from the methylene absorption bands by using the following relationships[10]:

$$\mathrm{PP} = S_{\alpha\alpha} \tag{1}$$

$$\mathrm{EP} = S_{\alpha\gamma} + S_{\alpha\delta}$$

$$\mathrm{EE} = 1/2\left(S_{\beta\delta} + S_{\delta\delta}\right) + 1/4S_{\gamma\delta}$$

Triad distributions were also analysed from both the methine and methylene absorptions using:

$$\mathrm{PPP} = T_{\beta\beta} \tag{2}$$

$$\mathrm{PPE} = T_{\beta\delta}$$

$$\mathrm{EPE} = T_{\delta\delta}$$

$$\mathrm{PEP} = S_{\beta\beta} = 1/2S_{\alpha\gamma}$$

$$\mathrm{EEP} = S_{\alpha\delta} = S_{\beta\delta}$$

$$\mathrm{EEE} = 1/2S_{\delta\delta} + 1/4S_{\gamma\delta}$$

From the dyad and triad distributions the monomer composition was calculated, since:

$$\mathrm{P} = \mathrm{PP} + 1/2\mathrm{PE} \tag{3}$$

$$\mathrm{E} = \mathrm{EE} + 1/2\mathrm{PE}$$

$$\mathrm{P} = \mathrm{PPP} + \mathrm{PPE} + \mathrm{EPE}$$

$$\mathrm{E} = \mathrm{EEE} + \mathrm{EEP} + \mathrm{PEP}$$

Table 3 lists dyad and triad concentrations for some of the fractions, and for comparison the corresponding values calculated from Bernouillian and first-order Markovian statistics. From this it can be seen that, with increasing elution temperature, the EP content is progressively reduced and by 105°C the EP content was 0.184; the fraction which separates at this temperature consisted mainly of long sequences of propylene units, i.e. [PPP] = 0.666, and long sequences of ethylene units, i.e. [EEE] = 0.205.

With increasing elution temperature, the content of long sequences of E units decreases, in that the EEE content of B12 is 0.103 and that of B13 is 0.056, while the content of long sequences of P increases. Above 115°C (B15), the fractions are mainly composed of long sequences of P units and are blocks of polypropylene with smaller amounts of ethylene blocks. At even higher elution temperatures the fraction is clearly polypropylene with no ethylene blocks.

The number-average sequence length of the blocks was derived from the relationships[10]:

$$\bar{n}_{\mathrm{E}} = \frac{[\mathrm{PP}] + \frac{1}{2}[\mathrm{PE}]}{\frac{1}{2}[\mathrm{PE}]} \tag{4}$$

$$\bar{n}_{\mathrm{E}} = \frac{[\mathrm{EE}] + \frac{1}{2}[\mathrm{PE}]}{\frac{1}{2}[\mathrm{PE}]}$$

From Bernouillian statistics:

$$n_{\mathrm{E}} = 1/\left(1 - P_{\mathrm{E}}\right), \quad n_{\mathrm{P}} = 1/P_{\mathrm{P}} \tag{5}$$

and first-order Markovian statistics:

$$n_{\mathrm{E}} = 1/P_{\mathrm{EP}}, \quad n_{\mathrm{P}} = 1/P_{\mathrm{PE}} \tag{6}$$

where n_{E} and n_{P} are the number-average sequence lengths of comonomer E and P; P_{E} and P_{P} are the probabilities of forming a macromolecular chain with monomer E or P as an active centre; and P_{EP} and P_{PE} are conditional probabilities of forming a chain with an active centre as EP* or PE*.

The number-average sequences of propylene and ethylene comonomer units are tabulated in *Table 4*. It can be seen that, except for B17 eluted at 120°C, all of the block copolymer fractions are block copolymers. Comparatively, the measured sequence distributions do not fit either a first-order Markovian or a Bernouillian model.

*FT*i.r. spectra ranging from 1600 to 600 cm^{-1} of the block copolymer fractions were measured. The 722 cm^{-1} peak is characteristic of the rocking vibration of methylene sequences[11], $-(CH_2)_n-$, with $n > 3$. The absorption at 722 cm^{-1} was used to measure the ethylene sequence content of each fraction; this content changes with eluting temperature, peaking at 60°C. The ethylene sequence content decreases with elution temperature for the fractions

Table 3 Sequence distribution in the fractions

Sequence	Observed value	Bernouillian model	Markovian model
(a) B11			
E	0.334	—	0.360
P	0.666	—	0.640
PP	0.574	0.444	0.484
EP	0.184	0.445	0.311
EE	0.334	0.112	0.204
PPP	0.569	0.295	0.367
PPE	0.043	0.296	0.235
EPW	0.082	0.074	0.038
PEP	0.055	0.148	0.067
EEP	0.074	0.149	0.177
EEE	0.205	0.037	0.116
(b) B12			
E	0.127	—	0.140
P	0.873	—	0.860
PP	0.857	0.762	0.830
EP	0.032	0.222	0.062
EE	0.111	0.016	0.108
PPP	0.855	0.665	0.800
PPE	0.009	0.194	0.060
EPE	0.009	0.014	0.001
PEP	0.008	0.097	0.007
EEP	0.016	0.028	0.048
EEE	0.103	0.002	0.084
(c) B13			
E	0.108	—	0.131
P	0.892	—	0.869
PP	0.862	0.796	0.812
EP	0.060	0.193	0.115
EE	0.078	0.012	0.074
PPP	0.818	0.710	0.758
PPE	0.028	0.172	0.107
EPE	0.047	0.010	0.004
PEP	0.009	0.086	0.025
EEP	0.043	0.021	0.064
EEE	0.056	0.001	0.041
(d) B15			
E	0.079	—	0.093
P	0.921	—	0.907
PP	0.904	0.848	0.875
EP	0.034	0.146	0.065
EE	0.062	0.006	0.060
PPP	0.879	0.781	0.843
PPE	0.021	0.134	0.063
EPE	0.021	0.006	0.001
PEP	0.011	0.067	0.012
EEP	0.011	0.012	0.042
EEE	0.056	0.001	0.039
(e) B17			
E	0.029	—	0.047
P	0.971	—	0.953
PP	0.950	0.943	0.914
EP	0.041	0.056	0.078
EE	~0	0.001	0.008
PPP	0.904	0.915	0.877
PPE	0.041	0.055	0.075
EPE	0.026	0.001	0.002
PEP	0.012	0.027	0.033
EEP	0.016	0.002	0.013
EEE	~0	~0	0.001

eluted above 65°C and, indeed, for those eluted above 110°C the E sequence content is essentially zero. These results suggest that the fractions obtained at the lowest elution temperatures are ethylene–propylene statistical copolymers; the fractions collected between 65 and 100°C contain long sequences and are block copolymers; while those obtained above 110°C are homopolymer polypropylenes.

The ratio of the absorbance at 998 to that at 973 cm^{-1} has been used to measure the distribution of propylene units in propylene–ethylene copolymers[12]. It can be seen from *Figure 2* that the propylene sequence content increases with elution temperature and the fractions obtained above 110°C are essentially polypropylene homopolymers.

In *Figure 3* the WAXD diffractograms of the fractions are compared. The fraction eluted at room temperature exhibits broad halos characteristic of liquid structures, while the

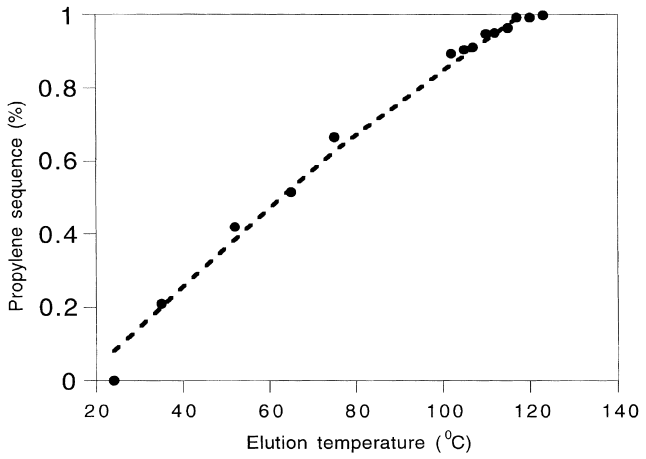

Figure 2 Variation of propylene sequence content with elution temperature

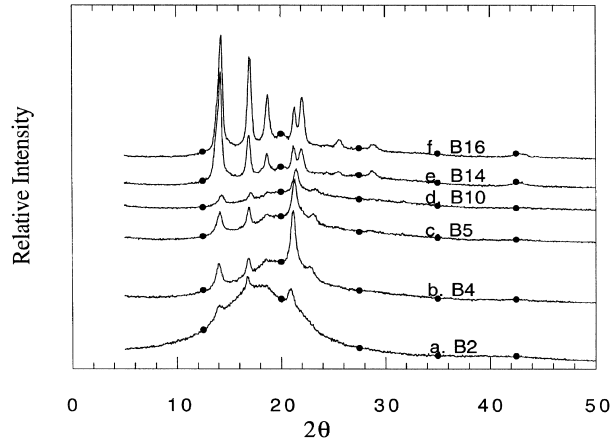

Figure 3 WAXD diffractogram of fractions eluted at different temperatures

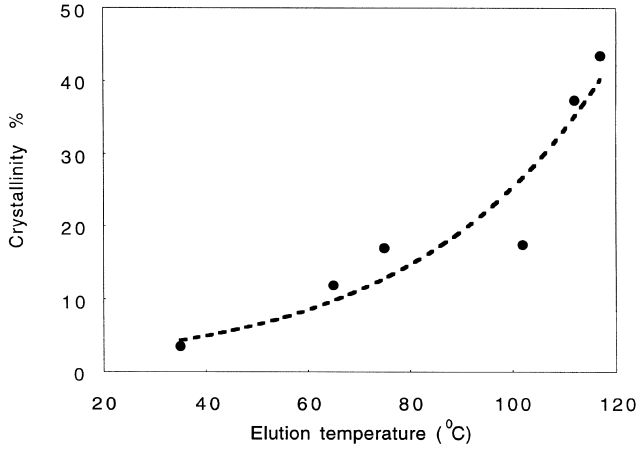

Figure 4 Variation of crystallinity with elution temperature

fractions eluted at progressively higher temperatures show progressively sharper crystalline peaks and reduced amorphous halos consistent with an overall increase in crystallinity.

Fractions B2, B4 and B5 have a diffraction line, at $2\theta = 23.4°$. This line is characteristic of PE and indeed can be assigned to the (2 0 0) plane of the PE crystal. In addition, these fractions exhibit diffraction lines at 14.15, 16.75, 18.60 and 21.90° characteristic of crystalline iPP. These fractions have sufficiently long E sequences for PE lamellae to form on crystallization. No diffraction line at 23.4° was found in fractions eluted below 65°C or above 110°C, so that the ethylene sequences in these fractions were not long enough to crystallise in sufficient concentrations to be detected by WAXD. This is consistent with both the ^{13}C-n.m.r. and *FT*i.r. spectroscopy analyses of the sequence distributions in these fractions.

WAXD can be also used to measure the volume fraction crystallinity, X_c, from the ratio of the areas under the crystalline and amorphous reflections, A_c and A_a:

$$X_c = \left[1 + \left(K_a A_a / K_c A_c\right)\right]^{-1} \quad (7)$$

where K_a and K_c are constants normally assumed to be equal. X_c was measured by assuming $K_a = K_c$ for each fraction. It can be seen from *Figure 4* that within the limited accuracy of this procedure there is a close relationship between the percentage crystallinity and the elution temperature of the fractions. This confirms that TREF fractionation of the block copolymer is based on the ability of the fractions to crystallise.

Combining the TREF weight distribution with the *FT*i.r. analysis of the fractions, it is apparent that the block copolymer is a blend of PP homopolymer, propylene–ethylene statistical copolymer (with negligible crystallinity), linear polyethylene, block propylene–ethylene copolymer and an isotactic polypropylene homopolymer.

Commercial block PP copolymers are invariably prepared in a two-step copolymerisation. The presence of PP homopolymer is obviously explained by production of the homopolymer in the first reactor, where only catalyst and propylene monomer are present. The propylene–ethylene copolymer is produced in the second stage, where ethylene and propylene are present, producing the copolymer. Any homopolymer polyethylene produced would result from transfer of the active site to ethylene monomer but would be limited by copolymerisation by the propylene.

WAXD, *FT*i.r. and ^{13}C-n.m.r. spectroscopic analyses suggest that the fraction eluted at room temperature is an amorphous statistical copolymer, i.e. an ethylene–propylene rubber (EPR). This contributes about 15% by weight to the bulk block copolymer. The fractions eluted above room temperature to 65°C are a PP-rich copolymer containing some E units, and contribute about 5% to the bulk copolymer. From 65 to 110°C, the fractions are mainly ethylene/propylene block copolymers with long P sequences and long E sequences. These contribute about 28% by weight to the bulk block copolymer. The E content of these blocks decreases with increasing eluting temperature, until they are effectively zero above 110°C. From 110 to 123°C, the fractions are composed mainly of P long sequences, i.e. PP isotactic homopolymer. This contributes about 52% by weight to the bulk block copolymer.

We conclude that from these studies that the commercial block copolymer is a complex blend of ethylene and propylene statistical and block copolymers and homopolymers.

Crystallisation behaviour

Dynamic d.s.c. crystallisation experiments were carried out in order to determine the temperature region in which each fraction crystallised. No crystallisation exdotherms were observed with fractions B1, B2 and B3. These samples only showed melting endotherms on reheating in the d.s.c., after slow cooling in the d.s.c. This clearly indicated that

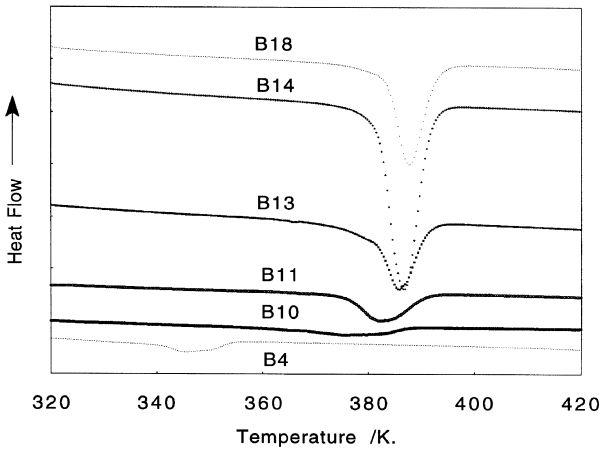

Figure 5 D.s.c. crystallisation trace for fractionated block propylene–ethylene copolymer fractions

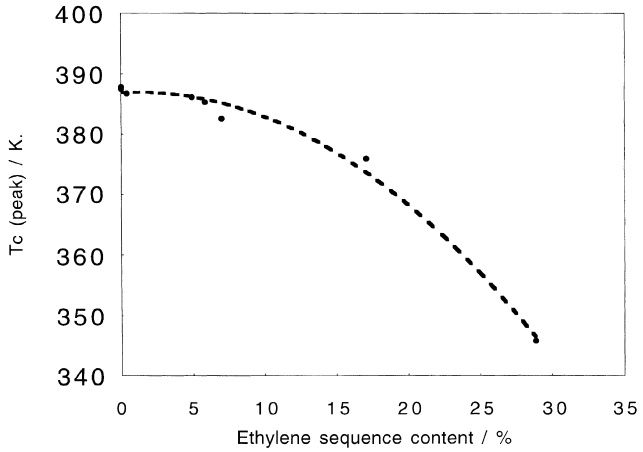

Figure 6 Effect of ethylene sequence content on crystallisation temperature (cooling rate: 10 K min^{-1})

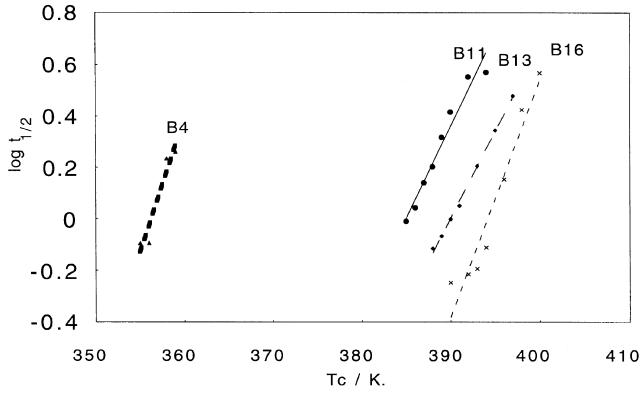

Figure 7 Variation of crystallisation half-life with temperature (ethylene content: B4, 29%; B11, 7%; B13, 5%; B16, 0%)

these samples are slow to crystallise and a low degree of crystallinity was observed.

Samples eluted above 65°C showed crystallisation exotherms on cooling in their d.s.c. curves, see *Figure 5*, but at different temperatures in line with their different comonomer content. The crystallisation temperature, T_c, decreased with increasing ethylene content, see *Figure 6*. A similar dependence was observed between ethylene content and crystallisation enthalpy, indicating that ethylene units were restricting the development of crystallinity.

D.s.c. can be used to measure the rate of heat evolution from a crystallising sample under isothermal conditions. Hay and co-workers[13,14] compared results obtained by d.s.c. and dilatometry on crystallising polyethylene and concluded that d.s.c. gave meaningful crystallisation data.

Assuming the fractional crystallinity, $X(t)$, can be evaluated by integrating the exotherm from the start to time t, i.e.

$$X(t) = \int_0^t \frac{dH}{dt}\,dt \Big/ \int_0^\infty \frac{dH}{dt}\,dt \tag{8}$$

the fractional extent of crystallinity with time is then analysed by the Avrami equation, such that

$$-\ln(1 - X_t) = Zt^n \tag{9}$$

The n value was determined by differentiating the above equation with respect to time:

$$n = -t\,dX_t'/dt/(1 - X_t')\ln(1 - X_t') \tag{10}$$

where X_t' refers to the fractional crystallinity of the primary crystallisation process. Z is determined from the half-life of the primary process, $t_{1/2}$: i.e. when $X_t' = 0.5$, $t = t_{1/2}$, then

$$Z = \frac{\ln 2}{t_{1/2}^n} \tag{11}$$

The primary crystallisation kinetics of block copolymer fractions with different ethylene contents were analysed. *Figure 7* shows plots of $\log(t_{1/2})$ against crystallisation temperature T_c for the block copolymer fractions with various ethylene contents. The crystallisation rate varied markedly with T_c and also with the ethylene content, in that fractions with less ethylene crystallised at higher temperatures and the crystallisation rates were reduced considerably by the increase of ethylene content.

The kinetic data of crystallisation were analysed by using[15]:

$$g = g_0 \exp\left(-\frac{\Delta E}{R(T_c - T_\infty)}\right) \exp\left(-\frac{K_g}{T_c(\Delta T)f}\right) \tag{12}$$

where g is proportional to $t_{1/2}^{-1}$, g_0 is a pre-exponential factor, $\Delta T = T_m^\circ - T_c$, ΔE is the activation energy for transport of polymer segments to the site of crystallisation, R is the gas constant, $T_\infty = T_g^\circ - 30$ K, K_g is a nucleation constant, and $f = 2T_c/(T_c + T_m^\circ)$.

The equilibrium melting temperature, T_m°, was evaluated by extrapolation of the melting temperature, T_m, with respect to the crystallisation temperature, T_c, according to the method of Hoffman and Weeks[16]. This treatment assumes that the nucleating and growth rates can be averaged.

From equation (12), we get:

$$\ln(g) + \frac{\Delta E}{R(T_c - T_\infty)} = \ln(g_0) - \frac{K_g}{fT_c\Delta T} \tag{13}$$

Figure 8 shows the plot of $[\ln(g) + \Delta E/R(T_c - T_\infty)]$ as a function of $1/T_c(\Delta T)f$, obtained from the experimental values of g, T_c, T_m and standard values of $\Delta E = 6280$ J mol^{-1} and $T_\infty = T_g - 30$ K = 239.6 K ([17]). Values for K_g and g_0 can be obtained directly from the graph, where the slope is $-K_g$ and the intercept is equal to $\ln(g_0)$. Once K_g is known, parameters characteristic of crystal growth can be determined.

Table 4 The degree of monomer dispersion and sequence length within the fractions

Fraction	Measured values		Bernouillian model		Markovian model	
	n_E	n_P	n_E	n_P	n_E	n_P
B11	4.63	7.24	1.502	2.99	2.32	4.12
B12	12.72	54.56	1.145	7.87	4.48	27.78
B13	3.60	29.73	1.121	9.26	2.28	15.15
B15	4.65	54.18	1.086	12.66	2.83	27.78
B17	1.00	47.34	1.030	34.48	1.20	24.39

Table 5 Values of the crystallographic unit-cell dimensions for polypropylene[27]

(1 1 0) growth plane	
a_0 (m)	5.49×10^{-10}
b_0 (m)	6.26×10^{-10}
$(a_0 b_0)$ (m^2)	3.43×10^{-19}

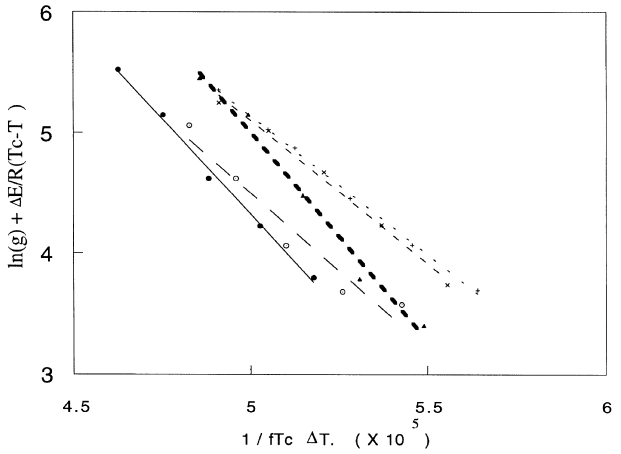

Figure 8 Relationship between $[\ln(g) + \Delta E/R(T_c - T_\infty)]$ and $1/fT_c\Delta T$ for block copolymer fractions at various T_c

K_g can be expressed as:

$$K_g = \frac{nb_0\sigma\sigma_e T_m^\circ}{\Delta h_f K} \quad (14)$$

where σ and σ_e are the lateral and end-surface free energies, respectively, of the growing crystal, b_0 is the molecular thickness and k is the Boltzmann constant. The value of n depends on the regime of crystallisation. At high temperatures (low undercooling) each occurrence of surface nucleation leads to rapid completion of the growth strip prior to the next nucleation event. This is referred to as regime I and $n = 4$. At lower temperature, in regime II, multiple surface nuclei form on the substrate and $n = 2$. When crystallisation occurs at still lower temperature, the separation between the multiple nuclei characteristic of regime II reaches its minimum value. This is regime III and $n = 4$.

By comparison with 18–20, it is assumed that all crystallisations in this work were carried out in Regime III. Thus:

$$K_g = \frac{4b_0\sigma\sigma_e T_m^\circ}{\Delta h_f k} \quad (15)$$

In determining σ_e, σ is estimated from:

$$\sigma = \alpha(a_0 b_0)^{1/2}\Delta h_f \quad (16)$$

where α was derived empirically to be 0.1, and is patterned after the Thomas–Stavely relationship[21]. The material constants for polypropylene used in the analysis are listed in *Table 5*.

Table 6 Kinetic parameters for the fractions

Sample	Ethylene content (%)	$K_g \times 10^{-5}$ (K^2)	σ_e (J m^{-2})
B11	7.0	3.456	0.0835
B13	5.8	3.168	0.0764
B14	0.4	2.571	0.0618
B16	0.0	2.374	0.0568
B17	0.0	2.301	0.0550

All of the kinetic parameters for the fractionated samples are listed in *Table 6*. As has already been reported[22], the surface free energy of the chain-folding surface in polymer crystals is connected directly with the degree of disorder in the amorphous overlayer. Increasing the disorder in the amorphous phase of the copolymers, due to increasing concentration of non-crystallizable co-units, is expected to increase the surface free energy of the crystals grown from the melt. As can be seen from *Table 6*, the surface free energy increased with increasing ethylene content. So, it is suggested that with increasing ethylene content, the degree of disorder in the copolymer is increased and the ability for crystallisation is reduced. This conclusion supports previous studies on X-ray diffraction and confirm that the TREF technique is successful for the copolymers.

Melting behaviour

Figure 9 shows the d.s.c. melting curves of the block fractions eluted above 65°C. For fraction B4 the first melting peak at lower temperature (~365 K) is attributed to a crystallisable copolymer, and the second peak (~391 K) to long ethylene sequences. On eluting from 102 to 110°C, the fractions consist of long propylene and long ethylene sequences, and the first melting peak at 390 K is attributed to the ethylene sequences while melting peaks at higher temperatures (410–440 K) are attributed to the P sequences. With increasing eluting temperature above 110°C, the lower-temperature peak becomes smaller and finally disappears. These fractions contain various amounts of ethylene and propylene blocks and their T_m° values were determined with Hoffman and Weeks' method[23–25], where T_m is plotted against T_c. The intersection of this straight line with the diagonal $T_c = T_m$ (representing equilibrium conditions) gives T_m°. *Figure 10* shows the relationship between ethylene sequence content, as measured by i.r. spectroscopy, and T_m° for the fractions. It can be seen that T_m° decreases with increasing ethylene sequence content. For the fractions eluted at high temperature, the ethylene content was almost zero but these fractions also had different T_m° such that the higher the eluting temperature, the higher the equilibrium melting point. It is suggested that this phenomenon arises from fractionation either by molecular weight or by degree of isotacticity of the PP homopolymer fractions.

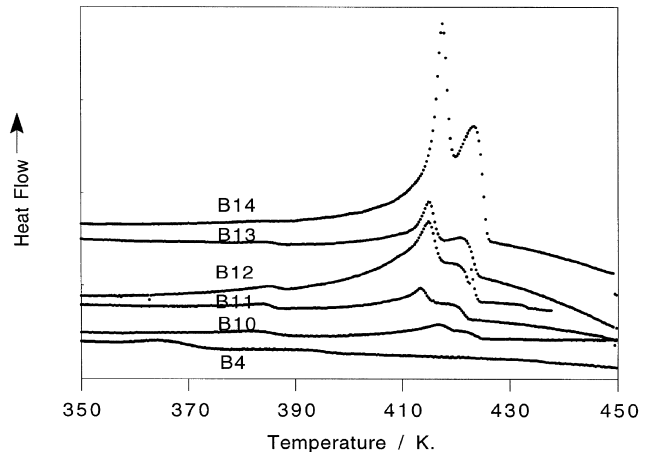

Figure 9 D.s.c. melting curves of block copolymer fractions

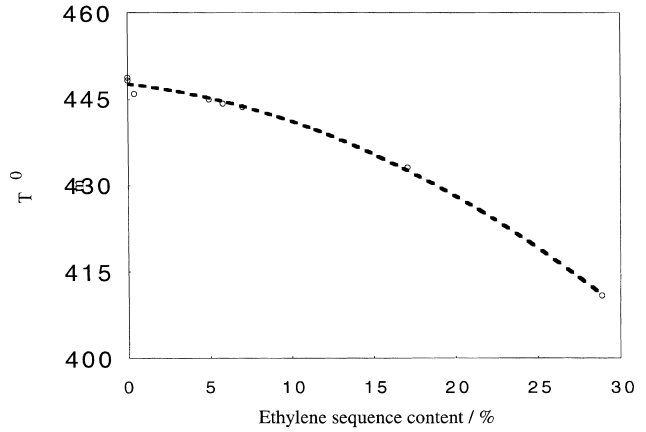

Figure 10 Relationship between ethylene sequence content and equilibrium melting point

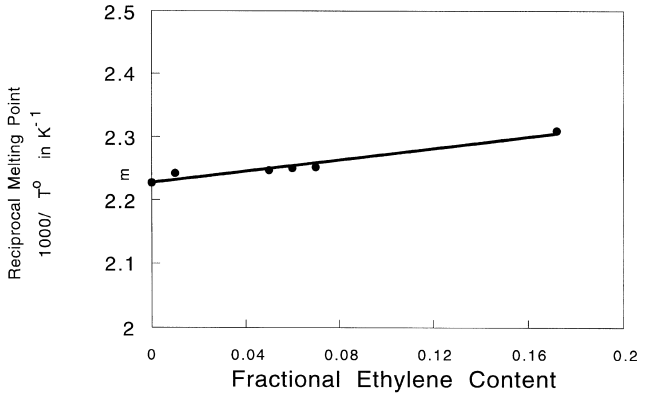

Figure 11 Dependence of the reciprocal equilibrium melting point on ethylene content

The simplest equation which relates the melting point of copolymers to composition is that of Flory[26], i.e.

$$\frac{1}{T_m} - \frac{1}{T_m^\circ} = -\frac{R}{\Delta H_m^\circ} \ln(x_a) \qquad (17)$$

The equation is derived from an equilibrium crystallisation model and is independent of lamellar thickness and morphology, but requires extrapolated equilibrium m.p. to be known. It assumes that the equilibrium values are lowered by a non-crystallisable comonomer unit, A, with a mole fraction, x_a. For small values of x_b, this becomes:

$$\frac{1}{T_m} - \frac{1}{T_m^\circ} = \frac{R}{\Delta H_m^\circ} \ln(x_b) \qquad (18)$$

where x_a is the mole fraction of crystallisable units of type A in the copolymer, and x_b represents the mole fraction of non-crystallisable comonomer incorporated in the chain. *Figure 11* shows the experimental data plotted as $1/T_m^\circ$ against x_a according to the above equation. An initial linear relationship was observed for the block copolymer fractions up to 15% ethylene content, but the intercept and slope corresponded to a value for T_m° of 449 ± 2 K and a heat of fusion of 18.5 kJ monomer mol^{-1} for isotactic polypropylene, compared with the expected values of 459 K and 8.79 kJ monomer mol^{-1} These values are clearly wrong and if the Flory relationship is valid for these copolymers, the ethylene units (which are depressing the m.p. in the copolymers) must be present as blocks.

CONCLUSIONS

A block propylene–ethylene copolymer was fractionated by the temperature rising elution fractionation (TREF) technique. The fractions were characterised by ^{13}C-n.m.r. spectroscopy, *FT*i.r. spectroscopy and WAXD. The results showed that the block copolymer studied in this work exhibits a complicated compositional heterogeneity, ranging from amorphous rubber-like copolymers (i.e. EPR) to polypropylene homopolymers. It was composed of about 15% amorphous EPR, 5% PP copolymer containing some ethylene units, 28% copolymer containing P long sequences and linear polyethylene, and 52% P long sequences or polypropylene homopolymer. The number-average sequences of P and E comonomers showed that the copolymer components had broad sequence distribution. First-order Markovian and Bernouillian models do not fit the sequence distribution. WAXD studies confirmed that the TREF fractionation occurs by separation of molecules by their crystallisability.

Crystallisation and melting behavior of the block copolymer fractions have been investigated. Dynamic crystallisation shows that the E content has a great influence on the crystallisation temperature region. With increasing E content the crystallisation temperature decreases.

Isothermal crystallisation kinetics were analysed with the Avrami equation for fractions. It has been found that the crystallisation rate varied markedly with crystallisation temperature T_c and also with the E sequence content in that fractions with less ethylene content crystallised at higher temperatures, and the crystallisation rates were reduced considerably by E sequence content. The Lauritzen–Hoffman equation was used to analyse the experimental data. It was found that the surface free energy, σ_e, increased with increasing E content; this suggests that the degree of disorder in the fractions increased, so that the tendency of crystallisation reduced.

Melting behavior was investigated for the block fractions. It was found that the equilibrium melting point, T_m°, decreased with increasing E content. The decrease of T_m° does not fit Flory's prediction. It has been suggested that the long E sequences in block fractions disrupted the crystallisation of long P sequences, and the long E sequences also crystallised.

ACKNOWLEDGEMENTS

Y. Feng is pleased to acknowledge the award of a research grant from the Sino–British Friendship Scholarship Scheme (SBFSS) during the tenure of this work.

REFERENCES

1. Jang, B. Z., Uhlman, D. R. and Vander Sande, J. B., *Polym. Eng. Sci.*, 1985, **25**, 643.
2. Jang, B. Z., Uhlman, D. R. and Vander Sande, J. B., *J. Appl. Polym. Sci.*, 1984, **29**, 3409.
3. Rybuikar, F. J., *J. Appl. Polym. Sci.*, 1969, **13**, 827.
4. Binsbergen, F. L. and Delarge, B. G. M., *Polymer*, 1970, **11**, 309.
5. Hoygshi, K., Morioka, T. and Toki, S., *J. Appl. Polym. Sci.*, 1993, **48**, 411.
6. Mirabella, F. M. and Ford, E. A., *J. Polym. Sci. (Phys.)*, 1987, **25**, 777.
7. Wild, L., Ryle, T. R., Knobeloch, D. C. and Peat, I. R., *J. Polym. Sci. (Phys.)*, 1982, **20**, 441.
8. Zhou, X. Q. and Hay, J. N., *Eur. Polym. J.*, 1993, **29**, 291.
9. Carman, C. J. and Wilkes, C. E., *Rubber Chem. Technol.*, 1971, **44**, 781.
10. Randall, J. C., *Polymer Sequence Determination*. Academic Press, New York, 1977.
11. Bucci, G. and Simonazzi, T., *J. Polym. Sci. (Part C)*, 1964, **7**, 203.
12. Ciampelli, F. and Valvassori, A., *J. Polym. Sci. (Part C)*, 1967, **16**, 377.
13. Mills, P. J. and Hay, J. N., *Polymer*, 1982, **23**, 1380.
14. Booth, A. and Hay, J. N., *Polymer*, 1969, **10**, 95.
15. Lauritzen, J. I. Jr. and Hoffman, J. D., *J. Appl. Phys.*, 1973, **44**, 4340.
16. Hoffman, J. D. and Weeks, J. J., *J. Res. Nat. Bur. Std—A Phys. Chem.*, 1962, **66A**(1), 13.
17. Janimak, J. J., Cheng, S. Z. D., Giusti, P. A. and Hsieh, E. T., *Macromolecules*, 1991, **24**, 2253.
18. Clark, E. J. and Hoffman, J. D., *Macromolecules*, 1984, **17**, 878.
19. Cheng, S. Z. D., Janimak, J. J., Zhang, A. and Cheng, H. N., *Macromolecules*, 1990, **23**, 298.
20. Goldfarb, L., *Makromol. Chem.*, 1978, **179**, 2297.
21. Thomas, D. G. and Stavely, L. A. K., *J. Chem. Soc.*, 1952, 4569.
22. Zachmann, H. G., *Pure Appl. Chem.*, 1974, **38**, 79.
23. Hoffman, J. D. and Weeks, J. J., *J. Res. Nat. Bur. Std*, 1962, **64A**, 73.
24. Kamide, K., Ohuo, K. and Kawai, T., *Makromol. Chem.*, 1970, **137**, 1.
25. Khanna, Y. P. and Kumar, R., *J. Polym. Sci. (Phys.)*, 1989, **27**, 369.
26. Flory, P. J., *Trans. Faraday Soc.*, 1955, **51**, 848.
27. Wunderlich, B., *Macromolecular Physics*, Vol. 1. Academic Press, New York, 1973.